

# Measuring and Rendering Art Paintings Using an RGB Camera

Shoji Tominaga and Norihiro Tanaka

Department of Informatics  
Osaka Electro-Communication University  
Neyagawa, Osaka 572-8530, Japan

---

## Abstract

*A method is proposed for measuring and rendering of art paints by using the simple system of an RGB camera only. The surface shape of an art painting is considered as a rough plane rather than a three-dimensional curved surface. Because the surface material has the dichromatic reflection property, the spectral reflectance function is estimated from the diffuse reflection component. First, we present an algorithm for estimating surface normal at each pixel point, based on an extended photometric stereo without using a rangefinder. Next, an algorithm is presented for estimating the spectral reflectance function from a set of RGB color values acquired at different illumination directions. Then, the surface reflectance and normal data are used for estimating the light reflection properties. The Torrance-Sparrow model is used for the model fitting and parameter estimation. Finally, an experiment using an oil painting is executed for demonstrating the feasibility of the proposed method.*

---

## 1. Introduction

A recent trend of the digital archives for art paintings is based on surface spectral information of the object surfaces (see 1,2). The spectral reflectance information is more important than color information for recording and rendering of paintings as digital images. In fact, an RGB color image is device-dependent and valid for only the fixed conditions of illumination and viewing. Therefore one cannot create an image of the same scene that will be seen under different illumination. On the other hand, once all surface-spectral reflectances are acquired, we can create images of the same scene under arbitrary illuminant.

However, the spectral reflectance information is not sufficient for rendering realistic images of such art objects as oil paintings. The surface material of the object consists of a thick oil layer. Although the surface is rough, gloss and highlight appear on the surface. Therefore we need some shape information of the object surface. A previous study 3 proposed a method using both the spectral data and the shape data. The shape data were acquired with a laser rangefinder and the spectral data were acquired with a multi-band camera. However, the laser rangefinder made unavoidable errors in measuring colored paintings including specularly, because it could measure a white matte surface with only dif-

fuse reflection component. Moreover, the multi-band camera with more than three sensors often encountered registration errors in exchanging color filters. As a result, we could not model the surface reflection properties for an art painting.

From a three-dimensional measurement viewpoint, Sato et al. 4 proposed a method for modeling shape and reflectance of a three-dimensional color-textured object. In their method, multiple color images were used to estimate the BRDF (bi-directional reflectance distribution function) of the object, which was digitized by a light striping range finder. Although this method eliminates problems with texture artifacts, they did not discuss the issue that of how to estimate surface spectral reflectance and how to correct for the alteration in color due to the light source and camera sensitivity function.

The present paper proposes a method for measuring and rendering of art paintings by using the simple system of a normal RGB camera only. Figure 1 depicts the flow for digital archives of art paintings from measurement to image rendering. Estimation of the surface-spectral reflectance function is an important stage. The surface of a painting has the dichromatic reflection property that light reflected from the surface is composed of two additive components, the body (diffuse) reflection and the interface (specular) reflection.

The spectral reflectance function is then estimated from the diffuse reflection component. We show that a reliable spectral reflectance can be estimated from a set of RGB color values acquired at different illumination directions.

The surface of an art painting can be considered as a rough plane rather than a three-dimensional curved surface. Therefore it is not necessary to reconstruct the three-dimensional surface for digital archiving. In this paper, surface normal is estimated at each pixel point, based on an extended photometric stereo, which uses the camera data at several illumination directions, without using a rangefinder.

The surface reflectance and normal data are then used for estimating the surface light reflection properties. We fit the Torrance-Sparrow model to those observed data and estimate the various model parameters. Finally, all the data are combined for rendering images of oil paintings with realistic shading effects under arbitrary conditions of illumination and viewing.

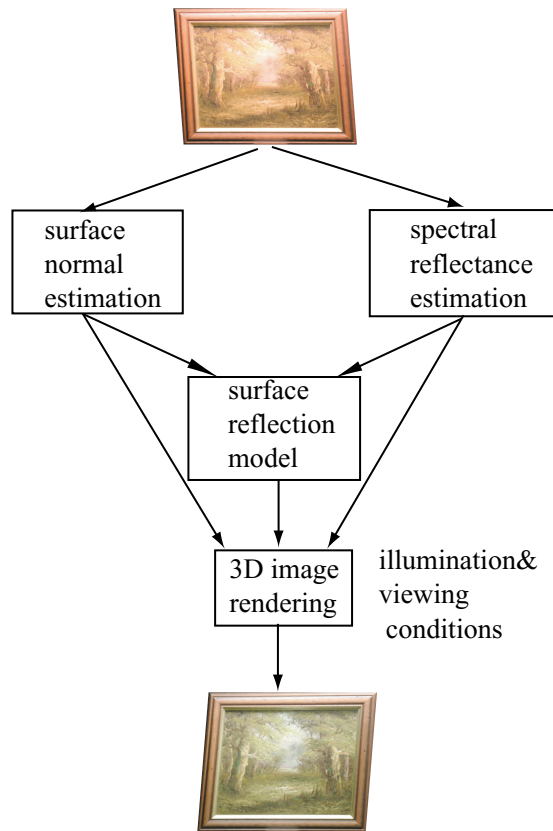


**Figure 1:** Flow from measurement to image rendering for art paintings.

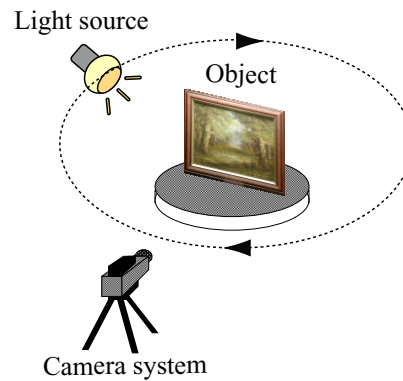
## 2. Measuring System

Figure 2 shows our system for measuring art paintings. The image data are obtained using an RGB digital camera (CANON D30) with a CMOS sensor. The number of pixels is about 3 MK (2160x1440), and the color value is sampled in 36 bits (12 bits per each color channel). First we examined the linearity of the camera response. Uniform color patches were measured with both the camera and a radiometer. By comparison of the camera outputs with the luminances of the incident light, the camera were determined to have a good linearity. The camera outputs for a diffuse reflection object are then described as

$$\rho_k = \int E(\lambda)S(x, \lambda)R_k(\lambda)d\lambda \quad (k = 1, 2, 3), \quad (1)$$

where  $E(\lambda)$  is the illuminant spectral-power distribution,  $S(x, \lambda)$  is the surface-spectral reflectance at the spatial location  $x$  on an object, and  $R_k(\lambda)$  is the spectral sensitivity functions of the sensor  $k$ . Accurate knowledge of the spectral sensitivity functions is needed for estimating the surface-spectral reflectance. We measured the camera spectral sensitivities by using a monochromator.

The image acquisition of the same object surface is repeated at different illumination directions as shown in Figure 3. Use of multiple illuminations has two advantages. First, the most suitable function of spectral reflectance without such noisy effects as specularity and shadowing can be selected from the image set observed under different illumination directions. Second, the surface normal vector at each pixel point can be estimated from a change in shading as the direction of a light source changes. In Figure 3 the angle of elevation is about 45-degree for all the light sources. Top means that the light source is right in the front of the object. The illumination direction was precisely determined using two specular mirrored balls.



**Figure 2:** Measuring system.

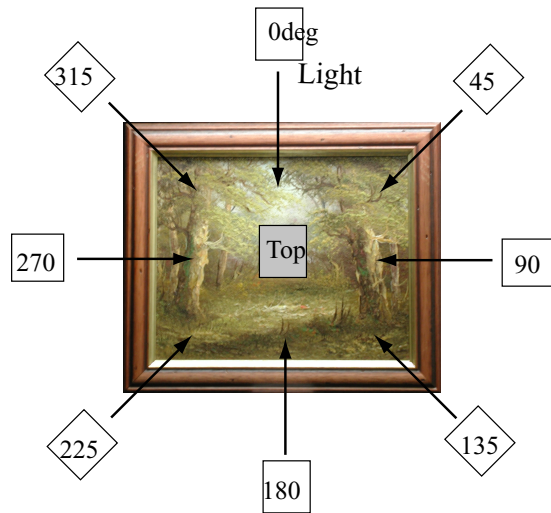


Figure 3: Imaging at different illumination directions.

### 3. Estimation of Surface Normals

#### 3.1. Basic idea

Photometric stereo can produce much denser descriptions of an object for a given camera resolution than binocular stereo because an estimate can be made at each pixel, rather than at object edges or the edges of projected stripes<sup>5,6,7</sup>. Here we present an extended photometric stereo method to compute the surface normal vector at each pixel of an observed art painting.

If an object surface is a perfect diffuser (Lambertian), the light intensity (radiance)  $I$  reflected from the surface illuminated by a light source is described as

$$I = \alpha \mathbf{N} \mathbf{l}_i, \quad (2)$$

where  $\mathbf{N}$  is a surface normal vector,  $\mathbf{l}_i$  is the illumination directional vector of  $i$ -th light source, and  $\alpha$  is the diffuse reflectance factor. Therefore the problem of estimating the three-dimensional vector  $\mathbf{N}$  can be solved using radiance values at three different illumination directions.

#### 3.2. Data selection

Now suppose that an object is observed at the illumination directions of nine angles of rotation around the optical axis as shown in Figure 3, where the elevation angle from the horizontal plane is fixed. In practice, the effects of specular highlights and shadows must be taken into account among the observed data set. We examine that each pixel is properly illuminated by the given light source. If the pixel belongs to specular highlight or shadow under the illumination, the corresponding camera data are discarded from the

observation set. Figure 4 shows an example of the camera outputs at one pixel that were obtained from a real painting for different illumination directions. The sensor numbers 0, 1, and 3 correspond to R, G, and B channels. The illumination direction numbers 0, 1, ..., 8 correspond to Top, 0, ..., 315 degrees. The separate red curve suggests that the observation by the direction 0 (Top) is specular highlight. Figure 5 depicts the averaged sensor outputs as a function of illumination direction. Therefore, a decision rule is determined as follows: Let  $\bar{\rho}_i$  be the average sensor value for  $i$ -th illumination direction, and  $\bar{\rho}$  be the average over the whole directions. If  $\bar{\rho}_i > w_1 \bar{\rho}$ , then the observation belongs to highlight. If  $\bar{\rho}_i < w_2 \bar{\rho}$ , then the observation belongs to shadow. The weights  $w_1$  and  $w_2$  represent threshold constants. In our experiment, we use  $w_1 = 1.2$  and  $w_2 = 0.1$ .

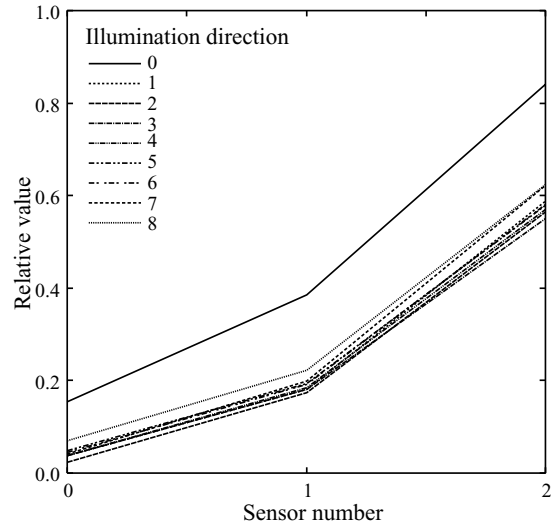


Figure 4: Example of camera outputs for different illumination directions.

#### 3.3. Estimation and correction

Let  $\mathbf{I} = [I_1, I_2, \dots, I_n]$  be a  $3 \times n$  matrix of the observed intensity values after eliminating the effects of specular highlights and shadows. In real estimation of normal vectors, we use the sensor output for only green channel as the radiance value. The assumption of diffuse reflection gives us the relationship of  $\mathbf{I} = \alpha \mathbf{N}^T \mathbf{L}$ , where  $\mathbf{L}$  is a  $3 \times n$  matrix showing a set of  $n$  illumination vectors.

For calibration, we use a standard white board as a reference white for correcting non-uniform illumination. Let  $W_1, W_2, \dots, W_n$  be the intensity values for the white board at  $n$  directions. We define an  $n$ -dimensional vector

$$\mathbf{W} = [W_1 / \cos(\theta_{w1}), W_2 / \cos(\theta_{w2}), \dots, W_n / \cos(\theta_{wn})], \quad (3)$$

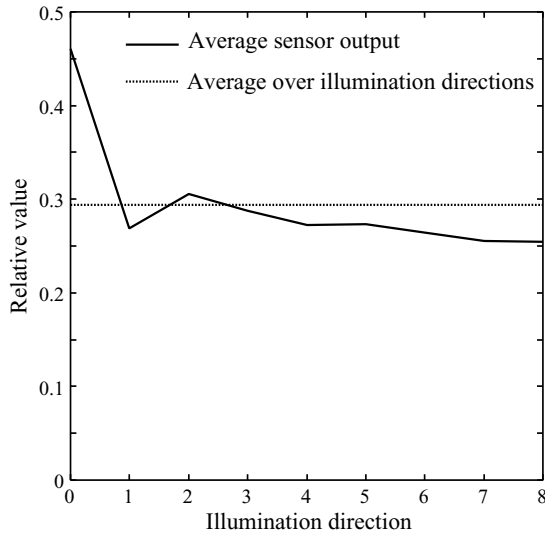


**Figure 5:** Plot of the averaged sensor outputs as a function of illumination direction.

where  $\theta_{w1}, \theta_{w2}, \dots, \theta_{wn}$  are the incident angles to the white board at each illumination direction. Then the correction is done by dividing the vector  $\mathbf{I}$  with  $\mathbf{W}$  in element-wise. Let  $\mathbf{I}'$  be the normalized vector of  $\mathbf{I}$ . The surface normal vector  $\mathbf{N}$  is obtained from the least squared solution as  $\mathbf{N} = \mathbf{I}'\mathbf{L}^+/\alpha$ , where  $\mathbf{L}^+$  is a generalized inverse of  $\mathbf{L}$ .

## 4. Estimation of Spectral Reflectance

### 4.1. Linear model representation

A linear finite-dimensional model is used to represent the surface spectral function. This model is effective in the sense that the number of unknown parameters can be reduced significantly when surface spectral reflectance functions with continuous spectra are represented by only a small number of basis functions. The spectral reflectance function  $S(x, \lambda)$  at a pixel point  $x$  can be expressed as a linear combination of  $n$  basis functions as

$$S(x, \lambda) = \sum_{i=1}^n \sigma_i(x) S_i(\lambda), \quad (4)$$

where  $\{S_i(\lambda), i = 1, 2, \dots, n\}$  is the set of basis functions for the reflectance, and  $\{\sigma_i(x)\}$  is the set of weights. The numbers of basis function,  $n$ , defines the model dimension for surfaces. Because the basis functions are known, given the above formulation in terms of linear models, the estimation problem becomes one of inferring the set of weight coefficients  $\{\sigma_i(x)\}$  from the camera outputs. As we use RGB three bands, the model dimension is limited to  $n = 3$ . A database of surface-spectral reflectances for about 500 different objects was used for our reflectance analysis. The

database consists of one set of 354 reflectances made by Vrhel et al. <sup>8</sup> and another set of 153 reflectances that we measured from different paint samples. The three principal components of the combined set of reflectances are selected as the basis functions  $\{S_i(\lambda), i = 1, 2, 3\}$  (see Figure 6).

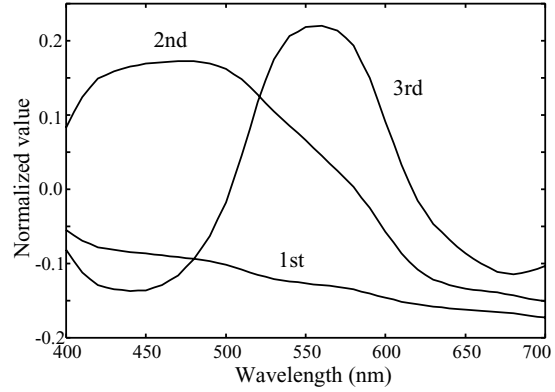


**Figure 6:** Basis functions for surface-spectral reflectances.

### 4.2. Estimation algorithm

A practical procedure for estimating  $\{\sigma_i(x)\}$  from the sensor outputs is summarized in the following (see <sup>9</sup>). We use the average of the camera outputs for different illumination directions after eliminating the highlight and shadow effects. The camera outputs are expressed using the linear model as

$$\rho_k = \sum_{i=1}^3 \sigma_i(x) \int E(\lambda) S_i(\lambda) R_k(\lambda) d\lambda. \quad (5)$$

Let  $\underline{\rho} (\equiv [\rho_i])$  be a three-dimensional column vector representing the camera outputs and  $\underline{\sigma} (\equiv [\sigma_i])$  be a three-dimensional column vector representing the reflectance coefficients. Moreover, define a  $3 \times 3$  matrix  $\mathbf{H} (\equiv [h_{ij}])$  with the element  $h_{ij} = \int E(\lambda) S_j(\lambda) R_i(\lambda) d\lambda$ . Then the sensor outputs are summarized in the matrix form  $\underline{\rho} = \mathbf{H}\underline{\sigma}$ . Note that  $h_{ij}$  are known ahead of time with the the illuminant spectrum, the basis functions of surface reflectance, and the camera spectral sensitivity functions. Therefore the reflectance vector at each pixel point can be obtained from the camera outputs as follows:

$$\hat{\underline{\sigma}} = \mathbf{H}^{-1} \underline{\rho}. \quad (6)$$

Finally, substituting the estimate into Eq. (4) recovers the spectral reflectance function in the form

$$\hat{S}(x, \lambda) = \hat{\sigma}_1(x) S_1(\lambda) + \hat{\sigma}_2(x) S_2(\lambda) + \hat{\sigma}_3(x) S_3(\lambda). \quad (7)$$



### 4.3. Correction

The final step is to correct the non-uniformity of illumination and the slant of reflecting surface. Again a standard white board is used as a reference white for calibrating non-uniform illumination. These corrections can be performed by the form

$$S'(x, \lambda) = (S(x, \lambda) / \cos(\theta_i)) / (W(x) / \cos(\theta_w)), \quad (8)$$

where  $\theta_i$  is the angle of light incidence at  $x$  on the object surface,  $\theta_w$  is the incidence angle at the corresponding location on the standard white board, and  $W(x)$  is a relative reflectance value of the white board.

## 5. Surface Reflection Model

### 5.1. Model description

The Torrance-Sparrow model <sup>10</sup> is used as a three-dimensional light reflection model for creating computer graphics images. This model is more precise than the Phong model <sup>11, 12</sup> in describing the specular reflection component. The spectral radiance is a function of the spatial location  $x$  and the wavelength  $\lambda$ , which is described as

$$Y(x, \lambda) = (\mathbf{N} \cdot \mathbf{L}) S'(x, \lambda) E(\lambda) + \beta \frac{D(\phi, \gamma) F(\theta_H, n) G}{\mathbf{N} \cdot \mathbf{V}} E(\lambda), \quad (9)$$

where the first and second terms represent, respectively, the diffuse and specular reflection components.  $\mathbf{V}$  is the view vector, and  $\phi$  is the angle between the vector  $\mathbf{N}$  and the bisector vector of  $\mathbf{L}$  and  $\mathbf{V}$ . The estimated spectral reflectance in the previous section is used as  $S'(x, \lambda)$  in the diffuse reflection term.  $E(\lambda)$  is the spectral distribution of illumination of an expected light source.

The specular reflection component in Eq.(9) consists of several terms: First,  $D$  is a function providing the index of surface roughness defined as  $\exp\{-\ln(2)\phi^2/\gamma^2\}$ , where the parameter  $\gamma$  is constant. Second,  $G$  is a geometrical attenuation factor. Third,  $F$  represents the Fresnel spectral reflectance, where  $\theta_H$  is the incidence angle to a micro facet and  $n$  represents the index of refraction. The surface material of a painting object can be regarded as an inhomogeneous dielectric material like plastic. The index of refraction is constant and the absorption coefficient is zero over the visible wavelength. We assume  $n = 1.45$  as the average of dielectric materials. Finally,  $\beta$  represents the intensity of the specular reflection component.

### 5.2. Estimation of model parameters

The roughness index  $\gamma$  and the specular intensity  $\beta$  are the unknown parameters to be estimated from the specular component of the image data of a painting. We already obtain

the spectral reflectance  $S'(x, \lambda)$  and the surface normal  $\mathbf{N}$  at each pixel. It is assumed that  $\gamma$  and  $\beta$  are constant over the whole surface of an objective painting. Since the specular component at any pixel has the same spectrum as the light source, the parameters are estimated based on the statistical distribution of the specular component.

The first step is to extract the specular component  $\rho_s$  at each pixel. This operation is done by the subtraction  $\rho_s = \rho_M - \rho_D$ , where  $\rho_M$  is the maximal sensor outputs among different illumination directions and  $\rho_D$  is the diffuse component that was determined in Section 3.2. The second step is a functional fitting to the normalized data of specular component at all pixels. We minimize the following fitting error over the whole image,

$$e = \min \sum_x \left\{ \left\| \rho_{Sx} \right\| \frac{(\mathbf{N}_x \cdot \mathbf{V}_x)(\mathbf{N}_x \cdot \mathbf{L}_x)}{G(\mathbf{N}_x, \mathbf{V}_x, \mathbf{L}_x) F(\theta_{Hx})} - \beta D(\phi_x, \gamma) \right\}^2, \quad (10)$$

where the subscript  $x$  of  $\rho_{Sx}$ ,  $\mathbf{N}_x$ ,  $\mathbf{V}_x$ ,  $\mathbf{L}_x$ ,  $\theta_{Hx}$ , and  $\phi_x$  denotes the vectors and angles at pixel point  $x$ . The above fitting error is a nonlinear function of  $\gamma$  and  $\beta$ . The parameters  $\gamma$  and  $\beta$  minimizing the function are solved as a least-squared solution of the nonlinear fitting problem. We use the Levenberg-Marquardt method for this solution.

## 6. Experimental Results

Figure 7 shows an oil painting used in our experiment. The object surface was illuminated by a flood lamp at nine directions and photographed by the RGB CMOS camera. The rectangular area Part 1 in Figure 7 indicates a part of rough surface including the trunks of a tree in the scene. This area was used for estimating the surface reflection model. First, Figure 8 shows an image rendering the estimation results of surface normals for Part 1. We can see big roughness at the edges of the trunk. These results are much more precise than the measurements by a laser range finder. Next, the surface-spectral reflectances were estimated at all pixel points. Especially, the accuracy of the estimates was examined at four areas in Figure 9. Figure 10 shows the estimated spectral curves, where red curves indicate the direct measurement results by using a spectroradio meter. A comparison between two curves in each graph suggests the reliability of the present spectral reflectance estimation based on only three color channels.

Third, Figure 11 shows an image consisting of only the extracted specular component for Part 1. After fitting the gauss function to the pixel distribution at a highlight peak region, we obtained the numerical values of  $\gamma = 0.075$  and  $\beta = 187$ . Finally, Figure 12 demonstrates the image rendering result under a fluorescent light source with the color temperature of D65. The vectors of illumination and view are  $\mathbf{L} = [0.00, 0.71, 0.71]^t$  and  $\mathbf{V} = [0.00, 0.00, 1.00]^t$ , respectively. We can see that the upper part of the image includes

specular highlights. For comparison, Figure 13 shows the observed image of the original painting under the real D65 fluorescent lamp and the same geometries of viewing and lighting. Both images provide a very close appearance. Although the present technique using surface normals cannot create the cast shadows, no problem happened to the image rendering under the usual conditions of viewing and lighting.



Figure 7: Oil painting of a natural scene.

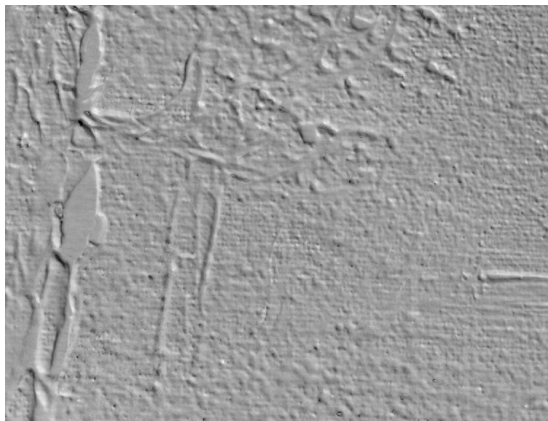


Figure 8: Image of the estimated surface normals.

## 7. Conclusions

This paper has proposed a method for measuring and rendering of art paints by using the simple system of a normal RGB camera only. The surface of an art painting was considered as a rough plane rather than a three-dimensional curved surface, so that it was not necessary to reconstruct the three-dimensional surface for digital archiving. Because the surface of a painting has the dichromatic reflection property, the spectral reflectance function is estimated from the

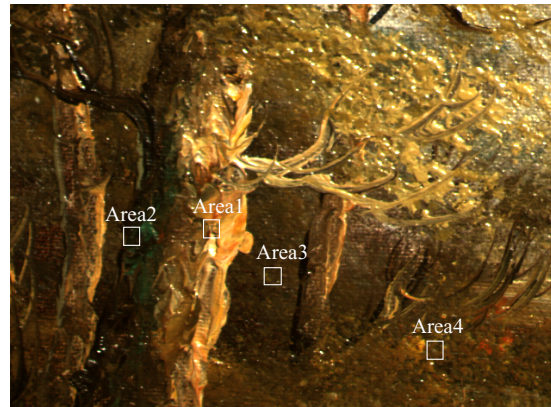


Figure 9: Accuracy check of the spectral reflectance estimates.

diffuse reflection component. We have shown that a reliable spectral reflectance can be estimated from a set of RGB color values acquired at different illumination directions. Surface normal was estimated at each pixel point, based on an extended photometric stereo without using a rangefinder. The surface reflectance and normal data were then used for estimating the light reflection properties. The Torrance-Sparrow model was fitted to the observed data so that the model parameters were estimated. Finally, an experiment using an oil painting was executed for demonstrating the feasibility of the proposed method.

## References

1. H. Maitre et al. Spectrophotometric image analysis of fine art paintings, *Proc. The 4th Color Imaging Conf. Color Science, Systems, and Applications*, 50-53, 1996. 1
2. Y. Miyake et al. Development of multiband color imaging systems for recording of art paintings. *Proc. SPIE: Color Imaging: Device-Independent Color, Color Hardcopy, and Graphic Arts IV*, 3648, 218-225, 1999. 1
3. S. Tominaga et al. 3D recording and rendering of art paintings, *Proc. The 4th Color Imaging Conf. Color Science, Systems, and Applications*, 337-341, 2001. 1
4. S. Sato et al. Object shape and reflectance modeling from observations. *SIGGRAPH '97 Proceedings*, 379-388, 1997. 1
5. K. Ikeuchi. Determining a depth map using dual photometric stereo, *Int. J. of Robotics Research*, 6(1), 15-37, 1987. 3
6. H. Rushmeier et al. Applying shape from lighting variation to bump map capture, *Proc. of the Eighth Eurographics Rendering Workshop*, 35-44, 1997. 3

7. H. Rushmeier et al. Acquiring input for rendering at appropriate levels of detail: Digitizing a Pieta. *Proc. of the Ninth Eurographics Rendering Workshop*, 81-92, 1998. 3
8. M.J. Vrhel et al. Measurement and analysis of object reflectance spectra, *Color Research and Application*, **19**, 4-9, 1994. 4
9. S. Tominaga. Multichannel vision system for estimating surface and illumination functions. *J. of Optical Society of America A*, **7**(2), 2163-2173, 1996. 4
10. K.E.Torrance and E.M.Sparrow. Theory for off-specular reflection from roughened surfaces. *J. of Optical Society of America A*, **57**(9), 1105-1114, 1967. 5
11. B.T. Phong, Illumination for computer-generated pictures. *Comm. ACM*, **18**(6), 311-317, 1975. 5
12. S. Tominaga et al, Estimation of Reflection Parameters from a Single Color Image, *IEEE Computer Graphics and Applications*, **20**(5), 58-66, 2000. 5

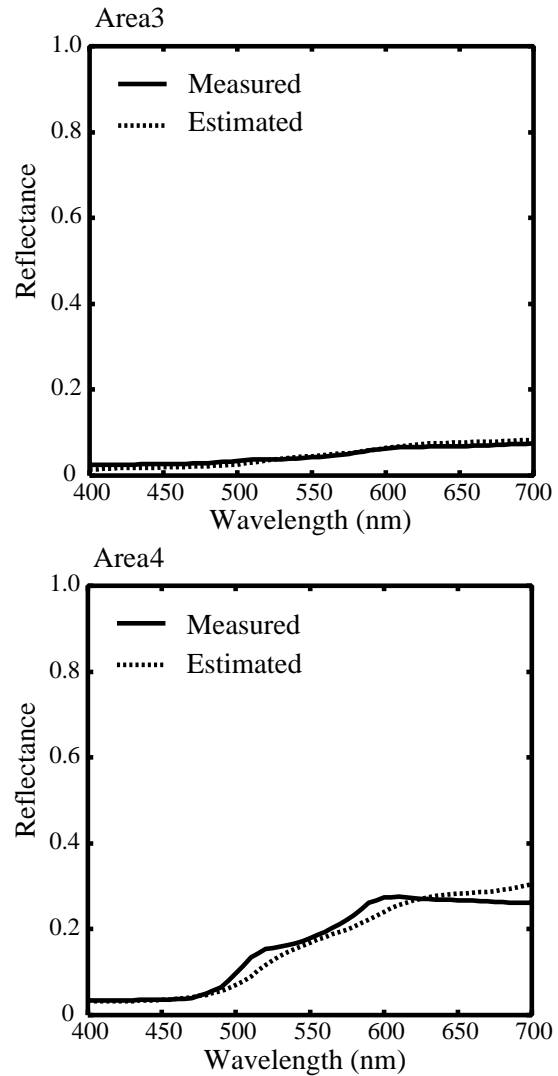
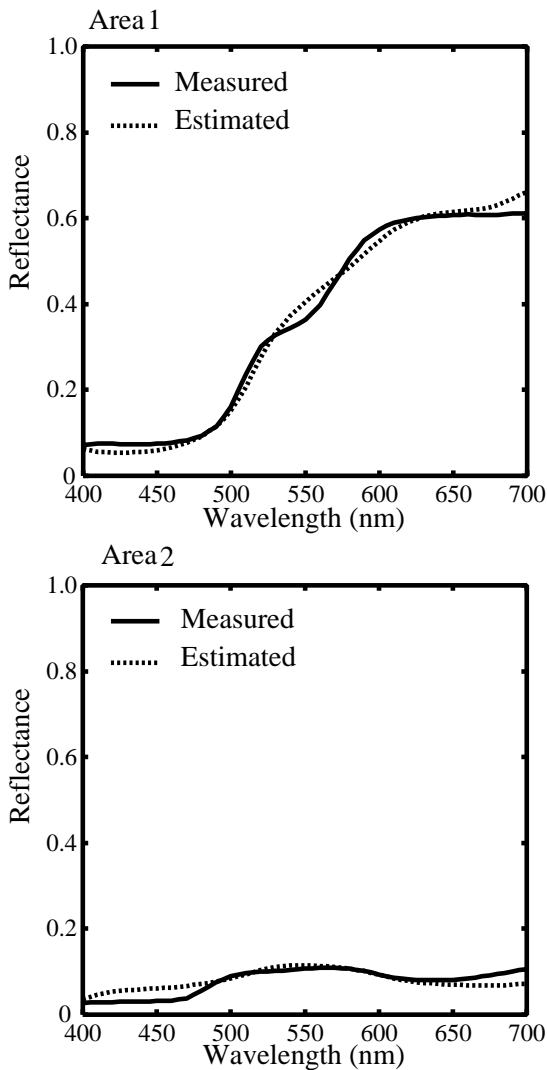


**Figure 10:** Estimation results of surface-spectral reflectances.





**Figure 11:** *Specular component image.*



**Figure 12:** *Image rendering result for a fluorescent light source with the color temperature of D65.*



**Figure 13:** *Observed image of the painting under the real D65 fluorescent lamp.*